

Thermal Diffusivity and Sound Velocity of Toluene Over a Wide Temperature Range¹

S. Will,^{2,3} A. P. Fröba,² and A. Leipertz²

The thermal diffusivity and the sound velocity of toluene have been determined in a wide temperature range up to the critical point by dynamic light scattering. Measurements were performed for both the liquid and the vapor phase at saturation conditions. The results obtained corroborate the usefulness of the technique for the determination of thermophysical properties. From the lack of reference data for the thermal diffusivity or other properties from which the thermal diffusivity may be derived in the high-temperature range and from deviations of experimental sound velocity data compared to values derived from the currently established equation of state, the need for further experimental investigations on this important reference fluid was established.

KEY WORDS: dynamic light scattering; sound velocity; thermal diffusivity; toluene.

1. INTRODUCTION

Dynamic light scattering (DLS) is a versatile technique for the determination of transport and other thermophysical properties [1, 2]. Due to its wide liquid range, toluene is an important reference fluid, especially for thermal conductivity and viscosity. Recently, we have determined the kinematic viscosity and surface tension of toluene over a wide temperature range by a modified surface light scattering technique [3]. This paper is an extension of earlier work from our laboratory on the thermal diffusivity of liquid toluene, which has been measured and published [4] previously.

¹ Paper presented at the Thirteenth Symposium on Thermophysical Properties, June 22–27, 1997, Boulder, Colorado, U.S.A.

² Lehrstuhl für Technische Thermodynamik (LTT), Friedrich-Alexander-Universität Erlangen-Nürnberg, Am Weichselgarten 8, D-91058 Erlangen, Germany

³ To whom correspondence should be addressed.

This investigation was intended as a test of the accuracy of the method, where the measured thermal diffusivity a was compared with values calculated from the relation $a = \lambda / (\rho c_p)$, where data for the thermal conductivity λ obtained by other methods and data for density ρ and isobaric heat capacity c_p from an equation of state were used. On the other hand, where the density is known accurately, data for the heat capacity may be deduced from a combination of a obtained by DLS and λ determined by other methods, e.g., by the transient hot wire technique [5]. In the present work, the temperature range of data for the liquid thermal diffusivity is extended up to the critical point and data for both the vapor thermal diffusivity and the sound velocity c_s in either phase are provided.

2. PRINCIPLE OF DYNAMIC LIGHT SCATTERING

The principle of DLS for the determination of thermophysical properties is given in detail elsewhere; see, e.g., Refs. 1, 2, 6, and 7. Here, only the essential features are repeated. DLS probes the spectrum of light scattered by a fluid in thermal equilibrium. This may be done using photon correlation by analyzing the temporal behavior of the scattered light signal. For the determination of the thermal diffusivity, the broadening of the central Rayleigh line of the spectrum is probed. With the exception of a region in the vicinity of the critical point, this is commonly done by applying a heterodyne technique, where a reference beam is added to the scattered light. In this case, the intensity correlation function is of the form

$$G^{(2)}(\tau) = A + B \exp(-\tau/\tau_{\text{cR}}) \quad (1)$$

with experimental constants A and B , where B is essentially determined by the ratio of scattered light and reference light and the coherence properties of the optical system. From the decay time τ_{cR} the diffusivity a may be calculated by

$$a = 1/(q^2\tau_{\text{cR}}) \quad (2)$$

where the modulus of the scattering vector \mathbf{q} ,

$$q = \frac{4\pi n}{\lambda_0} \sin \frac{\Theta}{2} \quad (3)$$

is given by the fluid refractive index n , the laser wavelength *in vacuo* λ_0 , and the scattering angle Θ . The decay time τ_{cR} can be reliably determined by a nonlinear fit to various lag-time intervals [8].

For the measurement of the sound velocity c_s one of the two Brillouin lines of the spectrum is probed, which are shifted in frequency and are symmetrical with respect to the Rayleigh line; c_s follows from $c_s = \omega q$, with ω being the frequency shift of the scattered light. Practically, ω is determined by adding a reference beam, which is shifted in frequency by means of an acoustooptical modulator with a given frequency shift similar to ω . In this case, the correlation function takes the form

$$G^{(2)}(\tau) = A + B \exp(-\tau/\tau_{cB}) \cos(\Delta\omega\tau) \quad (4)$$

where ω follows from the combination of the modulator frequency known and the residual mistuning $\Delta\omega$, which may be determined from the maximum in the Fourier transform of $G^2(\tau)$ [9].

3. EXPERIMENTAL PROCEDURE

The experimental setup used here is essentially the same as was employed in former investigations [7, 9]. The toluene sample under saturation conditions is included in a thermostated pressure vessel of cylindrical form, which is placed inside an insulated housing. The temperature is measured by a calibrated Pt-25 Ω probe assembled into the body of the vessel with an uncertainty of ± 0.005 K. Temperature stability is better than ± 0.01 K during an experimental run.

Light from an argon ion laser operating in a single longitudinal mode and at powers up to 300 mW at low temperatures is irradiated through a quartz window. The angle of incidence, which is defined as the angle between the optical axis of incidence and that of detection and from which the scattering vector can be deduced, is measured by back-reflection from a mirror, mounted to a precision rotation table. For imposing an additional reference beam, part of the incident light is reflected by a glass plate through a single modulator or a combination of modulators to realize the desired frequency shift. The detection optics consist simply of two circular stops with diameters of 1 and 2 mm. Scattered light is detected by two photomultiplier tubes taking the cross-correlation function in order to suppress afterpulsing effects. The signals are amplified, discriminated, and fed to a stand-alone correlator with 112 linearly spaced channels being operated with a sample time of 100 ns for the Brillouin measurements and with a sample time chosen in such a way that the correlation function covers about six decay times for the Rayleigh measurements.

The toluene sample was of spectroscopic grade with a specified purity of 99.9% and was used without further purification. Measurements were performed under saturation conditions in a temperature range from about

300 to 590 K in the liquid phase. For the vapor diffusivity, the temperature range started at 543 K. It should be emphasized that this lower limit is not a fundamental one, but with the laser power available, measurements at lower temperatures would require measurement times for a single run of about half an hour in order to obtain a reasonable statistical uncertainty. For the diffusivity in the liquid phase and for the sound velocity in both phases, the measurement times for a single run were typically of the order of 5 min, decreasing to 1 min for the highest temperatures in this study. At temperatures close to the critical point, the alignment of the setup became increasingly difficult due to density gradients and beam deflection within the sample cell. Thus, the investigation of the thermophysical properties in the vicinity of the gas-liquid critical point requires additional effort, which was not done here. For each temperature point, typically six single experimental runs were performed, where the laser irradiated the sample from either side with respect to the axis of observation in order to check for a possible misalignment.

4. RESULTS AND DISCUSSION

The results of our measurements are summarized in Tables I and II and Figs. 1–5. Sound velocity data can be well represented by a polynomial fit of the form

$$c_s = \sum_i a_i \left(\frac{T}{K} \right)^i \quad (5)$$

where c_s is in $\text{m} \cdot \text{s}^{-1}$, and the coefficients are given in Table III. For a good representation of the thermal diffusivity an additional term turned out to be necessary, which explicitly takes into account the critical part of the diffusivity and results in an equation of the form

$$a = \sum_{i=0}^4 a_i \left(\frac{T}{K} \right)^i + a_5 \left(\frac{T_c - T}{T_c} \right)^{0.67} \quad (6)$$

where a is in $10^{-8} \text{m}^2 \cdot \text{s}^{-1}$, and a_5 was approximated as an additional constant, and the critical temperature was taken as $T_c = 593.95 \text{K}$ [10].

Our first interest is directed to the liquid thermal diffusivity for a comparison with earlier work performed by DLS [4]. Figure 2 shows the difference between the fit of our data and that of other reference data, where the measurements of both Hendrix et al. [11] and Kraft et al. [4] were also performed by DLS, and those of Wang and Fiebig [12] by forced Rayleigh scattering. For a comparison with data from thermal conductivity

Table I. Experimental Values of the Thermal Diffusivity a of Toluene Under Saturation Conditions

Liquid phase		Vapor phase	
T (K)	a ($10^{-8} \text{ m}^2 \cdot \text{s}^{-1}$)	T (K)	a ($10^{-8} \text{ m}^2 \cdot \text{s}^{-1}$)
298.15	8.75	543.15	20.07
323.15	8.11	545.65	19.25
348.15	7.43	548.15	18.27
373.15	6.85	550.65	17.38
393.15	6.53	553.15	16.54
398.15	6.41	555.65	15.55
413.15	6.16	558.15	14.66
423.15	5.96	560.65	13.86
433.15	5.78	563.15	13.05
443.15	5.66	565.65	12.07
448.15	5.50	568.15	11.35
453.15	5.45	570.65	10.49
460.65	5.33	573.15	9.43
463.15	5.33	575.65	8.44
473.15	5.21	578.15	7.61
483.15	5.09	580.65	6.34
485.65	5.05	583.15	5.36
493.15	5.05	585.15	4.70
498.15	4.90	585.65	4.51
510.65	4.79	587.15	3.68
523.15	4.67	588.15	3.03
528.15	4.66	589.15	2.55
535.65	4.54		
543.15	4.43		
548.15	4.37		
553.15	4.33		
558.15	4.24		
560.65	4.09		
563.15	4.11		
568.15	3.97		
573.15	3.83		
575.65	3.62		
578.15	3.46		
580.65	3.24		
583.15	2.94		
584.15	2.85		
585.15	2.66		
586.15	2.49		
587.15	2.24		
588.15	2.01		
589.15	1.89		
590.15	1.55		
591.15	1.31		

Table II. Experimental Values of the Sound Velocity c_s of Toluene Under Saturation Conditions

Liquid phase		Vapor phase	
T (K)	c_s ($\text{m} \cdot \text{s}^{-1}$)	T (K)	c_s ($\text{m} \cdot \text{s}^{-1}$)
323.15	1195.1	463.15	184.4
348.15	1092.1	473.15	180.7
373.15	992.4	483.15	177.8
398.15	896.4	493.15	175.0
423.15	798.8	503.15	171.4
433.15	761.5	513.15	167.4
443.15	723.8	518.15	165.2
453.15	685.4	523.15	162.1
463.15	649.4	528.15	159.5
473.15	612.3	533.15	156.5
483.15	575.3	538.15	153.4
493.15	534.4	543.15	149.5
503.15	499.7	548.15	146.1
513.15	460.5	553.15	141.6
523.15	420.6	558.15	137.7
533.15	382.5	560.65	135.1
543.15	336.7	563.15	133.1
553.15	296.4	565.65	130.2
563.15	252.3	568.15	127.5
573.15	202.8	570.65	124.9
575.65	190.2	573.15	122.3
578.15	176.2	575.65	118.7
580.65	163.0	578.15	114.8
583.15	148.9	580.65	112.2
585.65	134.2	583.15	108.4
		584.15	106.3
		585.65	103.9
		587.15	102.0
		588.15	100.9
		589.15	98.20
		590.15	96.95
		591.15	95.69

measurements with the transient hot-wire method [13–16] and the regression by Ramirez et al. [17], these data have again been converted, with c_p and ρ from Goodwin's equation of state [10], into the thermal diffusivity. At temperatures above 450 K there is an increasing difference between our data and the DLS measurements by Kraft et al. [4] that is outside the combined uncertainty. The most likely reason for the discrepancy may be

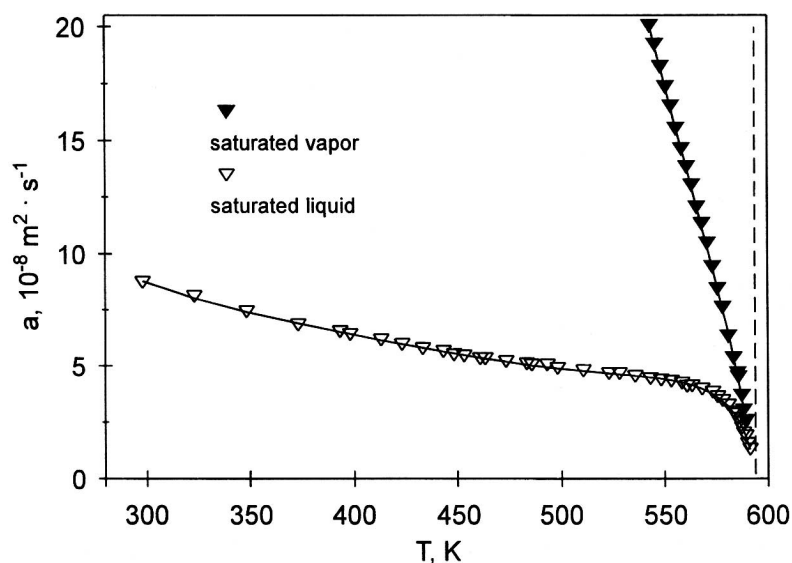


Fig. 1. Thermal diffusivity of toluene under saturation conditions.

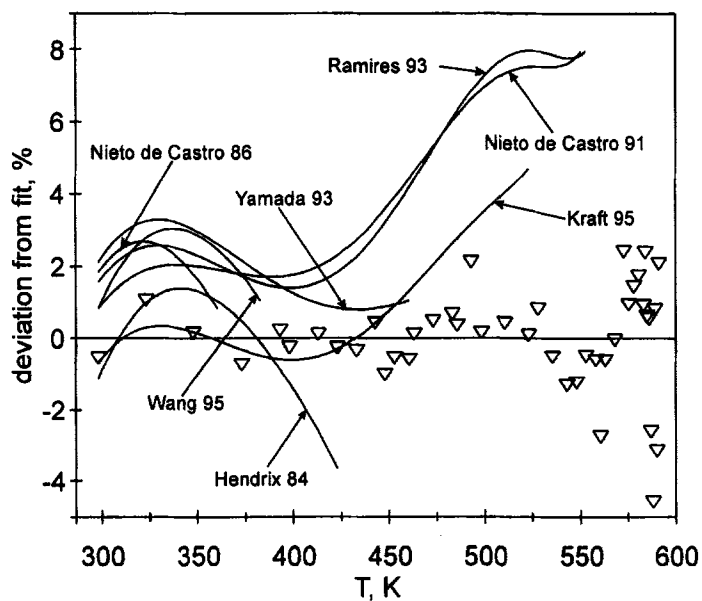


Fig. 2. Thermal diffusivity of liquid toluene: deviations of experimental data from this work (∇) and of literature results from the fit according to Eq. (6).

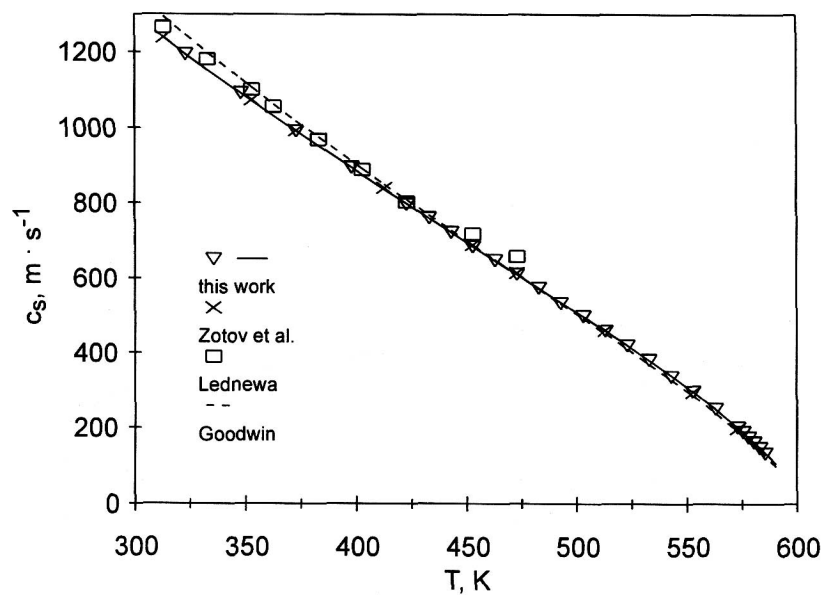


Fig. 3. Sound velocity of liquid toluene.

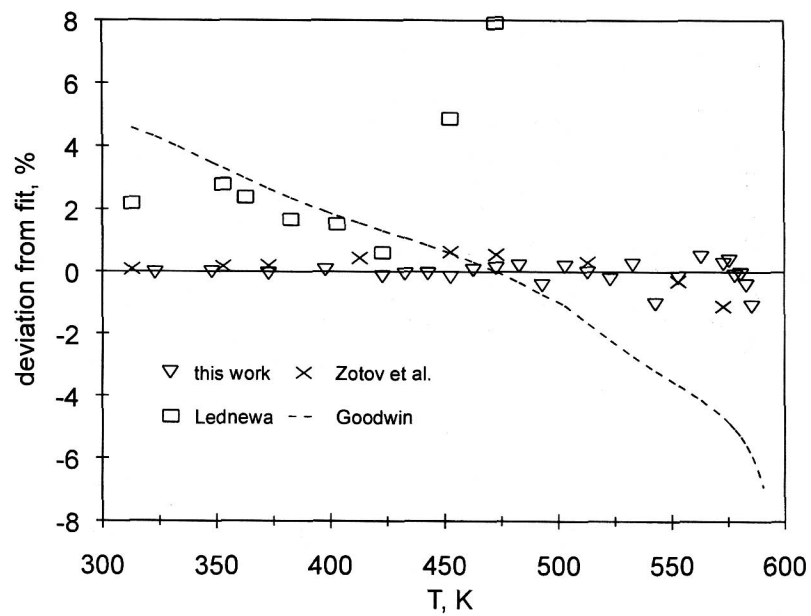


Fig. 4. Sound velocity of liquid toluene: deviations of experimental data from this work (∇) and of literature results from the fit according to Eq. (5).

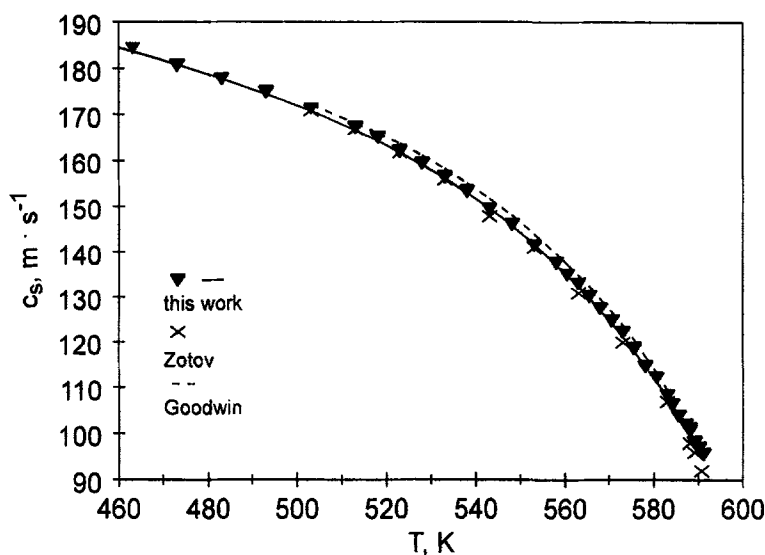


Fig. 5. Sound velocity of gaseous toluene.

found in the definition of the thermodynamic state. Probably, in the relevant temperature range the older measurements were not taken under saturation conditions, but in the compressed liquid phase, with an increasing deviation from saturation pressure with temperature leading to an increase in thermal diffusivity. In order to check our present data, we carried out four completely independent measurement series at a temperature of 473 K, with new samples within the cell and a new adjustment of the setup. These measurements agreed within $\pm 0.5\%$. For the higher-temperature range there is a pronounced deviation from the regression of Ramires et al.,

Table III. Coefficients of Eqs. (5) and (6)

	Eq. (6) thermal diffusivity a		Eq. (5) sound velocity c_s	
	Liquid phase	Vapor phase	Liquid phase	Vapor phase
a_0	-12.312	3,941.7	10,181	-7,464.8
a_1	-0.682544	-20.23016	-94.738	64.6066
a_2	2.970774×10^{-3}	0.0347411	0.4284658	-0.20425524
a_3	-4.954328×10^{-6}	-1.99638×10^{-5}	$-1.0139902 \times 10^{-3}$	2.8764095×10^{-4}
a_4	3.271235×10^{-9}	0	1.202641×10^{-6}	-1.529194×10^{-7}
a_5	105.259	84.51	-5.70687×10^{-10}	—

which is verified only up to temperatures of 553 K. There might, however, be suspicion about the heat capacity values at these high temperatures. Finally, the standard deviation of our measurements became clearly worse at higher temperatures. The root mean square deviation of our data from the fit according to Eq. (6) is 1.4% for the whole temperature range. It reduces to 0.7% when only data below 550 K are taken into account but, accordingly, increases to 2% for temperatures above 550 K. Excluding a fundamental q -dependence in this temperature range still considerably apart from the critical point, the main reason may be found in an increasing experimental difficulty. We cannot completely suppress temperature gradients within the cell because of the large difference from ambient temperature and the necessity for an optical access. Even small deviations from the nominal temperature may result in a considerable relative error in this region. Here, future measurements should incorporate an additional possibility for temperature control of the air close to the cell windows.

Due to long measurement times at lower temperatures, the data for thermal diffusivity in the vapor phase had to be restricted to temperatures above 540 K. Again, the uncertainty of our measurements increases toward high temperatures, where the average deviation from the fit is 2.3% for temperatures above 580 K, compared to 0.6% for temperatures below 580 K and 1.3% for the whole temperature range.

For liquid-phase sound velocities our experimental values may be compared with values from the equation of state (EOS) of Goodwin [10] and with the experimental data of Zotov et al. [18] and Lednewa [19] obtained by acoustical measurements. There is excellent agreement between our data and those of Zotov et al., yet a joint systematic deviation compared with the EOS. Our experimental values can be reproduced by the fit with a root mean square error of 0.37%; again, there is an increase in scatter, from 0.13% below 540 K to 0.45% above 540 K. It should be noted that the measured sound velocities are naturally not in the thermodynamic $\omega=0$ limit, and thus, dispersion might affect both average values and standard deviations. In our experiments, such effects have not been observed, but in further studies they should be given more thorough consideration.

For gas-phase sound velocities, qualitatively similar statements hold as for vapor diffusivity regarding the range of temperatures covered and the standard deviations of the fits. An excellent average deviation of 0.3% was obtained for the whole range of temperatures covered, with a value of 0.2% below 580 K and 0.4% above this temperature. The maximum deviation from the EOS sound velocities is 2%. The data of Zotov [20] deviate by -4% from our values at the highest temperatures, where good agreement between our data and EOS values is found.

5. CONCLUSION

We have shown that dynamic light scattering may be utilized to measure thermal diffusivities and sound velocities of fluids over a wide temperature range. Values for toluene have been determined in both the gas and the liquid phases. A comparison of results obtained for the thermal diffusivity in the high-temperature range was not possible due to the lack of other data sets in this region. Here, experiments by other techniques would be most helpful, especially for the thermal conductivity and the isobaric heat capacity. Additionally, more experimental data for the sound velocity would be desirable, as the present results indicate deviations from the currently established equation of state. Moreover, also further DLS experiments may be performed in the vicinity of the critical point, where additional effort is necessary due to the large temperature gradients between the sample and ambient conditions. Finally, the data presented here may motivate a comparison of experimental techniques, especially in the high temperature region and for thermal conductivity and diffusivity.

REFERENCES

1. J. N. Shaumeyer, R. W. Gammon, and J. V. Sengers, in *Measurement of the Transport Properties of Fluids*, W. A. Wakeham, A. Nagashima, and J. V. Sengers, eds. (Blackwell Scientific, Oxford, 1991), pp. 197–213.
2. A. Leipertz, *Fluid Phase Equil.* **125**:219 (1996).
3. A. P. Fröba, S. Will, and A. Leipertz, *Appl. Opt.* **36**:7615 (1997).
4. K. Kraft, M. Matos Lopes, and A. Leipertz, *Int. J. Thermophys.* **16**:423 (1995).
5. M. Matos Lopes, M. L. V. Ramires, C. A. Nieto de Castro, K. Kraft, A. Leipertz, and R. A. Perkins, *Proc. Fourth Asian Thermophys. Prop. Conf., Tokyo* (1995), p. 795.
6. S. Will and A. Leipertz, in *Diffusion in Condensed Matter*, J. Kärger, ed. (Vieweg, Wiesbaden, 1998), pp. 153–178.
7. K. Kraft and A. Leipertz, *Int. J. Thermophys.* **15**:387 (1994).
8. S. Will and A. Leipertz, *Appl. Opt.* **32**:3813 (1993).
9. K. Kraft and A. Leipertz, *Appl. Opt.* **32**:3886 (1993).
10. R. D. Goodwin, *J. Phys. Chem. Ref. Data* **18**:1565 (1989).
11. M. Hendrix, A. Leipertz, M. Fiebig, and G. Simonsohn, *Int. J. Heat Mass Transfer* **30**:333 (1987).
12. J. Wang and M. Fiebig, *Heat Mass Transfer* **31**:83 (1995).
13. C. A. Nieto de Castro, S. F. Y. Li, A. Nagashima, and W. A. Wakeham, *J. Phys. Chem. Ref. Data* **15**:1073 (1986).
14. R. A. Perkins, H. M. Roder, and C. A. Nieto de Castro, *J. Res. Natl. Inst. Stand. Technol.* **96**:247 (1991).
15. C. A. Nieto de Castro, R. A. Perkins, and H. M. Roder, *Int. J. Thermophys.* **12**:985 (1991).
16. T. Yamada, T. Yaguchi, Y. Nagasaka, and A. Nagashima, *High Temp. High Press.* **25**:513 (1993).

17. M. L. V. Ramires, C. A. Nieto de Castro, and R. A. Perkins, *High Temp. High Press.* **25**:269 (1993).
18. V. V. Zotov, B. N. Kireev, and Yu. A. Neruchev, *Zh. Prikl. Mekh. Tekh. Fiz.* **1975**:162 (1975).
19. T. M. Lednewa, *Vestn. Mosk. Univ.* **11**:49 (1956).
20. V. V. Zotov, *Uch. Zap. Kursk. Gos. Pedagog. Inst.* **54**:63 (1969).